Vol. 2, No. 3, 2012, 35–44

Shahrood University of Technology

Journal of Solid and Fluid Mechanics

Optimal discrete-time control of robot manipulators in repetitive tasks

M. M. Fateh[1,*] and M. Baluchzadeh[2]

[1] Professor, Shahrood University of Technology
[2] M.Sc. Student, Shahrood University of Technology

Abstract

Optimal discrete-time control of linear systems has been presented already. There are some difficulties to design an optimal discrete-time control for a robot manipulator since the robot manipulator is highly nonlinear and uncertain. This paper presents a novel robust optimal discrete-time control for electrically driven robot manipulators in performing repetitive tasks. The robot performs repetitive tasks by tracking a periodic trajectory. The proposed controller includes a discrete linear quadratic controller and a time-delay controller. To apply the discrete linear quadratic controller, a novel nominal model is obtained for the robotic system which is discrete, linear, and time-invariant. Then, nonlinearities and uncertainties of the robotic system are compensated by the robust time-delay controller. The proposed control law is verified by stability analysis and its effectiveness is illustrated by simulations. Recently, time-optimal and minimum-norm discrete repetitive control of robot manipulators has been proposed. Compared with it, the proposed control has an advantage of being free from manipulator dynamics, thus it is simpler, more robust, and less computational with smoother control efforts.

Keywords: Optimal discrete repetitive control; Discrete linear quadratic control; Time-delay control; Robot manipulators.

1. Introduction

A promising control approach to achieve tracking of periodic signals is repetitive control. It has gained a great deal of research interest in various forms of control approaches for the robot manipulators such as discrete time repetitive control [1], repetitive model reference adaptive control [2], Lyapunov-based repetitive learning control [3] and adaptive repetitive learning control [4].

The mentioned control approaches are based on the model of robot manipulator; however, the model uncertainty is compensated. Industrial robots meet the key structural features such as repeatability, which is important in many manufacturing applications for performing repetitive trajectories. Therefore, model-based control may work in tracking repetitive trajectories. However, performance of the control system depends on the precision of model. This characteristic plays an important role particularly in the high-speed and high-accuracy applications. The higher orders un-modeled dynamics will degrade the control performance in the high speed. It is well known that a robot manipulator is highly nonlinear, heavily coupled and multivariable, thus shows a complicated imprecise model affected by uncertainties. Therefore, finding a control approach that is less dependent on model or free of model will be very useful. Alternatively, robust and adaptive control may be proposed to overcome uncertainties.

Iterative learning control can efficiently cancel the repetitive error [5]. However, its performance is degraded by the non-repetitive errors. In addition, learning rules may show low rate of convergence and unsatisfactory performance in the initial trials. The control system is affected by initial conditions [6], disturbances [7], learning transient [8] and non-minimum phase systems [9]. Performance of the repetitive control has been efficiently improved by utilizing adaptive control [10-12]. However, adaptive control may be involved in computational complexity, unsatisfactory initialization and implementation difficulty. Adaptive iterative learning control has been proposed to remove some mentioned shortcomings [13]. An iterative term is used to cope with unknown

* Corresponding author, Phone: (+98)273-3393116
Email: mmfateh@shahroodut.ac.ir

parameters and disturbances. The control design is simple and robust; however, it has low rate of convergence and unsatisfactory performance in the initial trials.

So far, torque control strategy is a commonly used strategy for robot manipulators. However, there would be some shortcomings to apply this strategy since the torque control laws are affected by manipulator dynamics to become highly nonlinear, heavily coupled and computationally extensive. In contrast, voltage control strategy [14] can be free from manipulator dynamics. Actually, the robot control becomes the problem of motor control in the voltage control strategy. This advantage provides a simple control design in a decentralized structure, thus makes it superior to the torque control strategy. In comparison with voltage control in [14], a fully feedback linearization is not applied in this paper. The proposed control law is simple with an advantage of not using the motor current and its time derivative. Following our research on voltage control strategy, some voltage control laws were proposed for electrically driven robots in the form of robust fuzzy control [15], robust task-space control [16], robust time-delay control [17], robust adaptive control [18], Robust Time-Optimal Minimum-Norm Discrete Repetitive (RTOMNDR) control [19] and adaptive fuzzy estimation of uncertainty [20].

Based on the voltage control strategy, this paper presents a novel Robust Optimal Discrete Repetitive (RODR) control for electrically driven robot manipulators. Despite nonlinearity of manipulator dynamics, as a novelty, a discrete linear time-invariant model for the robotic system is introduced. All nonlinearity, unmodeled dynamics, parametric uncertainty and external disturbances in the robotics system are given as a lumped uncertainty in the model. Then, a two-term control law is proposed in which the first term is a Discrete Linear Quadratic (DLQ) controller to provide an optimal control and guarantee the system stability. The second term is a robust time-delay controller to compensate the lumped uncertainty for improving performance of the control system.

The rest of this paper is organized as follows: Section 2 introduces a discrete linear time-invariant model for the robotic system. Section 3 presents a robust time-delay control law. Section 4 describes the DLQ controller. Section 5 presents the stability analysis. Section 6 illustrates the simulation results and gives comparisons with the RTOMNDR control. Finally, Section 7 concludes the paper.

2. Discrete Linear Time Invariant Model

Consider a rigid robot manipulator driven by permanent magnet dc motors [21]. The voltage equation of permanent magnet dc motors in the matrix form is given by

$$\mathbf{v} = \mathbf{R}\mathbf{I_a} + \mathbf{L}\dot{\mathbf{I}}_\mathbf{a} + \mathbf{k_b}\dot{\boldsymbol{\theta}}_\mathbf{m} \tag{1}$$

where $\mathbf{v} \in R^n$ is the vector of motor voltages, $\mathbf{I_a} \in R^n$ is the vector of motor currents and $\boldsymbol{\theta}_\mathbf{m} \in R^n$ is the vector of motor positions. $\mathbf{k_b}, \mathbf{R}, \mathbf{L} \in R^{n\times n}$ are the diagonal matrices of the back emf constants, resistances and inductances, respectively. Matrices and vectors are presented in the bold form.

The motor torque is produced by the motor current as

$$\boldsymbol{\tau}_\mathbf{m} = \mathbf{K_m}\mathbf{I_a} \tag{2}$$

where $\boldsymbol{\tau}_\mathbf{m} \in R^n$ is the vector of motor torques and $\mathbf{K_m} \in R^{n\times n}$ is the diagonal matrix of torque constants.

The motor position vector $\boldsymbol{\theta}_\mathbf{m}$ is related to the joint position vector of robot manipulator $\mathbf{q}$ through the gears as

$$\mathbf{q} = \mathbf{r}\boldsymbol{\theta}_\mathbf{m} \tag{3}$$

where $\mathbf{r} \in R^{n\times n}$ is the diagonal matrix of reduction gear coefficients.

The electric motors drive the robot manipulator according to the dynamics

$$\mathbf{J_m}\ddot{\boldsymbol{\theta}}_\mathbf{m} + \mathbf{B_m}\dot{\boldsymbol{\theta}}_\mathbf{m} + \mathbf{r}\boldsymbol{\tau} = \boldsymbol{\tau}_\mathbf{m} \tag{4}$$

where $\boldsymbol{\tau} \in R^n$ is the vector of joint torques, $\mathbf{J_m}, \mathbf{B_m} \in R^{n\times n}$ are the diagonal matrices of motor inertia and damping, respectively.

Dynamics of a robotic manipulator is given by

$$\mathbf{D}(\mathbf{q})\ddot{\mathbf{q}} + \mathbf{C}(\mathbf{q},\dot{\mathbf{q}})\dot{\mathbf{q}} + \mathbf{g}(\mathbf{q}) = \boldsymbol{\tau} \tag{5}$$

where $\mathbf{D}(\mathbf{q}) \in R^{n\times n}$ is the inertia matrix, $\mathbf{C}(\mathbf{q},\dot{\mathbf{q}})\dot{\mathbf{q}} \in R^n$ is the vector of generalized centripetal and Coriolis forces, and $\mathbf{g}(\mathbf{q}) \in R^n$ is the vector of generalized gravitational forces.

By using (1)-(5), the dynamics of robotic system including the robot manipulators and electric motors is then expressed as

$$\begin{aligned}&\mathbf{R_a}\mathbf{K_m^{-1}}\left(\mathbf{J_m}\mathbf{r}^{-1} + \mathbf{r}\mathbf{D}(\mathbf{q})\right)\ddot{\mathbf{q}} + \\ &\left(\mathbf{R_a}\mathbf{K_m^{-1}}\mathbf{B_m}\mathbf{r}^{-1} + \mathbf{R_a}\mathbf{K_m^{-1}}\mathbf{r}\mathbf{C}(\mathbf{q},\dot{\mathbf{q}}) + \mathbf{K_b}\mathbf{r}^{-1}\right)\dot{\mathbf{q}} \\ &+ \mathbf{R_a}\mathbf{K_m^{-1}}\mathbf{r}\mathbf{g}(\mathbf{q}) + \mathbf{L}\dot{\mathbf{I}}_\mathbf{a} + \boldsymbol{\xi} = \mathbf{V}\end{aligned} \tag{6}$$

The vector $\boldsymbol{\xi} \in R^n$ denotes the external disturbances. The obtained model is highly nonlinear, heavily coupled, multivariable and uncertain. In order to obtain a simple discrete linear time-invariant model, all nonlinearities and uncertainties including un-modeled dynamics, parametric uncertainty and external disturbances are given as the lumped uncertainty. For this purpose, we rewrite (6)

$$\mathbf{R_a K_m^{-1} J_m r^{-1} \ddot{q}} + \left(\mathbf{R_a K_m^{-1} B_m r^{-1} + K_b r^{-1}}\right)\mathbf{\dot{q}} + \boldsymbol{\varphi} = \mathbf{V} \tag{7}$$

where $\boldsymbol{\varphi}$ is given by

$$\boldsymbol{\varphi} = \mathbf{R_a K_m^{-1} r D(q) \ddot{q} + R_a K_m^{-1} r C(q, \dot{q}) \dot{q}} + \mathbf{R_a K_m^{-1} r g(q) + L \dot{I}_a} + \boldsymbol{\xi} \tag{8}$$

Then, one can rewrite (7) by using nominal terms as

$$\mathbf{\hat{R}_a \hat{K}_m^{-1} \hat{J}_m \hat{r}^{-1} \ddot{q}} + \left(\mathbf{\hat{R}_a \hat{K}_m^{-1} \hat{B}_m \hat{r}^{-1} + \hat{K}_b \hat{r}^{-1}}\right)\mathbf{\dot{q}} + \boldsymbol{\psi} = \mathbf{V} \tag{9}$$

where $\boldsymbol{\psi}$ is called the lumped uncertainty expressed as

$$\left(\mathbf{R_a K_m^{-1} J_m r^{-1} - \hat{R}_a \hat{K}_m^{-1} \hat{J}_m \hat{r}^{-1}}\right)\mathbf{\ddot{q}} + \left(\mathbf{R_a K_m^{-1} B_m r^{-1} - \hat{R}_a \hat{K}_m^{-1} \hat{B}_m \hat{r}^{-1} + K_b r^{-1} - \hat{K}_b \hat{r}^{-1}}\right)\mathbf{\dot{q}} + \boldsymbol{\varphi} = \boldsymbol{\psi} \tag{10}$$

and $\mathbf{\hat{R}_a}$, $\mathbf{\hat{K}_m}$, $\mathbf{\hat{J}_m}$, $\mathbf{\hat{r}}$ and $\mathbf{\hat{K}_b}$ are the nominal coefficient matrices for the real matrices $\mathbf{R_a}$, $\mathbf{K_m}$, $\mathbf{J_m}$, $\mathbf{r}$ and $\mathbf{K_b}$, respectively.

One can easily form a state-space model for the robotic system (9),

$$\mathbf{\dot{X}} = \mathbf{MX} + \mathbf{NV} - \mathbf{N}\boldsymbol{\psi} \tag{11}$$

where the state matrix $\mathbf{M}$, the input gain matrix $\mathbf{N}$ and state vector $\mathbf{X}$ are expressed as

$$\mathbf{X} = \begin{bmatrix} \mathbf{q} \\ \mathbf{\dot{q}} \end{bmatrix}, \ \mathbf{N} = \begin{bmatrix} \mathbf{0} \\ \mathbf{\hat{r} \hat{J}_m^{-1} \hat{K}_m \hat{R}_a^{-1}} \end{bmatrix}, \quad \mathbf{M} = \begin{bmatrix} \mathbf{0} & \mathbf{I} \\ \mathbf{0} & -\mathbf{\hat{r} \hat{J}_m^{-1} \hat{K}_m \hat{R}_a^{-1}}\left(\mathbf{\hat{R}_a \hat{K}_m^{-1} \hat{B}_m \hat{r}^{-1} + \hat{K}_b \hat{r}^{-1}}\right) \end{bmatrix} \tag{12}$$

where $\mathbf{I}$ is the identity matrix.

There exists a vector $\mathbf{V_d}$ such that

$$\mathbf{\dot{X}_d} = \mathbf{MX_d} + \mathbf{NV_d} \tag{13}$$

where $\mathbf{X_d} = \begin{bmatrix} \mathbf{q_d} \\ \mathbf{\dot{q}_d} \end{bmatrix}$ and $\mathbf{q_d}$ is a desired joint position vector. $\mathbf{V_d}$ is calculated by

$$\left(\mathbf{N}^T \mathbf{N}\right)^{-1} \mathbf{N}^T \left(\mathbf{\dot{X}_d} - \mathbf{MX_d}\right) = \mathbf{V_d} \tag{14}$$

Subtracting (11) from (13) results in the state-space model in the tracking space as,

$$\mathbf{\dot{E}} = \mathbf{ME} + \mathbf{NU} + \mathbf{N}\boldsymbol{\psi} \tag{15}$$

where

$$\mathbf{E} = \mathbf{X_d} - \mathbf{X} \tag{16}$$

$$\mathbf{U} = \mathbf{V_d} - \mathbf{V} \tag{17}$$

The proposed model (15) has an advantage that $\mathbf{M}$ and $\mathbf{N}$ are constant and free from manipulator parameters. However, model (15) includes the uncertainty $\boldsymbol{\psi}$. The proposed model is an uncertain linear time-invariant system.

Using a sampling period σ, substituting $k\sigma$ into t, then approximating $\mathbf{\dot{E}}$ as $\mathbf{\dot{E}} = (\mathbf{E}(t+\sigma) - \mathbf{E}(t))/\sigma$ in (15), we obtain a discrete linear time-invariant system of the form

$$\mathbf{E}_{k+1} = \mathbf{AE}_k + \mathbf{BU}_k + \mathbf{B}\boldsymbol{\psi}_k \tag{18}$$

where $\mathbf{E}_k = \mathbf{E}(k\sigma)$, $\mathbf{A} = \mathbf{I} + \sigma\mathbf{M}$, $\mathbf{B} = \sigma\mathbf{N}$, $\mathbf{U}_k = \mathbf{U}(\sigma k)$, $\boldsymbol{\psi}_k = \boldsymbol{\psi}(k\sigma)$.

3. Robust Time-Delay Control Law

We have proposed this type of uncertainty estimation to estimate the uncertainty in the robust impedance control of a hydraulic suspension system [22], the control of flexible-joint robots [17] and the RTOMNDR control [19].

To make the dynamics of tracking error well-defined such that the robot can track the desired trajectory, we make the following assumptions:

Assumption 1: *The desired trajectory* $\mathbf{q_d}$ *must be smooth in the sense that* $\mathbf{q_d}$ *and its derivatives up to a necessary order are available and all uniformly bounded.*

Smoothness of the desired trajectory can be guaranteed by proper trajectory planning.

As a necessary condition to design a robust controller, the matching condition must be satisfied:

Matching condition: *the uncertainty must enter the system the same channel as the control input.* Then, the uncertainty is said to satisfy the matching condition [23] or equivalently is said to be matched. We ensure the matching condition since in system (15), the lumped uncertainty $\boldsymbol{\psi}$ enters the system the same channel as the control input $\mathbf{U}$.

As a necessary condition to design a robust control, the external disturbance $\boldsymbol{\xi}$ used in (6) must be bounded. Thus, the following assumption can be made.

Assumption 2: *The external disturbance* $\boldsymbol{\xi}$ *is bounded as*

$$\|\boldsymbol{\xi}\| \le \xi_{\max} \tag{19}$$

where $\xi_{\max}$ is a positive constant.

The voltage of every motor should be limited to protect the motor against over voltages. For this purpose, every motor is equipped with a voltage limiter. Therefore, we introduce the following assumption:

Assumption 3: *The motor voltages are bounded as*

$$\|\mathbf{V}\| \le V_{\max} \tag{20}$$

where $V_{\max}$ is a positive constant.

A two-term control law is proposed to track the repetitive trajectory in the workspace. The first term is an optimal DLQ controller and the second term is a robust time-delay controller. Thus, system (18) is presented as

$$\mathbf{E}_{k+1} = \mathbf{AE}_k + \mathbf{BU}_{1,k} + \mathbf{BU}_{2,k} + \mathbf{B\psi}_k \tag{21}$$

where $\mathbf{U}_{1,k}$ and $\mathbf{U}_{2,k}$ are the first and second terms of control input. Performance of the repetitive control is improved if the lumped uncertainty $\mathbf{\psi}_k$ is compensated. The uncertainty is perfectly compensated if

$$\mathbf{BU}_{2,k} = -\mathbf{B\psi}_k \tag{22}$$

Since $\mathbf{\psi}_k$ is not known, control law (18) cannot be defined. To estimate the uncertainty, we obtain from (21)

$$\mathbf{B\psi}_k = \mathbf{E}_{k+1} - \mathbf{AE}_k - \mathbf{BU}_{1,k} - \mathbf{BU}_{2,k} \tag{23}$$

Since $\mathbf{E}_{k+1}$ is not available in the kth step, $\mathbf{B\psi}_k$ cannot be calculated. Instead, the previous value of $\mathbf{B\psi}_k$ is used as

$$\mathbf{B\psi}_{k-1} = \mathbf{E}_k - \mathbf{AE}_{k-1} - \mathbf{BU}_{1,k-1} - \mathbf{BU}_{2,k-1} \tag{24}$$

The term $\mathbf{B\psi}_{k-1}$ can be calculated since all terms in the RHS of (24) are known and available. Thus, we propose a robust control law

$$\mathbf{BU}_{2,k} = -\mathbf{B\psi}_{k-1} \tag{25}$$

We express the second term in the control law by substituting (24) into (25) to yield

$$\mathbf{BU}_{2,k} = -\mathbf{E}_k + \mathbf{AE}_{k-1} + \mathbf{BU}_{1,k-1} + \mathbf{BU}_{2,k-1} \tag{26}$$

4. Discrete Linear Quadratic Controller

The Discrete Linear Quadratic (DLQ) controller has been efficiently used as an optimal controller in discrete linear systems. Substituting (26) into (21) yields

$$\mathbf{E}_{k+1} = \mathbf{AE}_k + \mathbf{BU}_{1,k} + \mathbf{B}\left(\mathbf{\psi}_k - \mathbf{\psi}_{k-1}\right) \tag{27}$$

In order to apply the DLQ, a nominal model in the form of discrete linear system is suggested from (27) as

$$\mathbf{E}_{k+1} = \mathbf{AE}_k + \mathbf{BU}_{1,k} \tag{28}$$

Then, the DLQ controller is given by

$$\mathbf{U}_{1,k} = -\mathbf{K}_k \mathbf{E}_k \tag{29}$$

The gain matrix $\mathbf{K}_k$ is calculated by minimizing a given cost function of the form [24]

$$L = 0.5\mathbf{E}_N^*\mathbf{SE}_N + 0.5\sum_{k=0}^{N-1}\left\{\begin{array}{l}\left(\mathbf{E}_k^*\mathbf{QE}_k + \mathbf{U}_{1,k}^*\mathbf{RU}_{1,k}\right) + \\ \mathbf{\lambda}_{k+1}^*\left(\mathbf{AE}_k + \mathbf{BU}_{1,k} - \mathbf{E}_{k+1}\right) + \\ \left(\mathbf{AE}_k + \mathbf{BU}_{1,k} - \mathbf{E}_{k+1}\right)^*\mathbf{\lambda}_{k+1}\end{array}\right\} \tag{30}$$

with respect to $\mathbf{E}_k$, $\mathbf{U}_{1,k}$ and $\mathbf{\lambda}_k$, where $\mathbf{\lambda}_k$ is the Lagrange multiplier, $\mathbf{Q}$ and $\mathbf{R}$ are symmetric positive definite matrices. As a result,

$$\mathbf{K}_k = [\mathbf{R} + \mathbf{B}^*\mathbf{p}_k\mathbf{B}]^{-1}\mathbf{B}^*\mathbf{p}_k\mathbf{A} \tag{31}$$

where $\mathbf{p}_k$ is calculated as

$$\mathbf{p}_k = \mathbf{Q} + \mathbf{A}^*\mathbf{p}_{k-1}\mathbf{A} - \mathbf{A}^*\mathbf{p}_{k-1}\mathbf{B}[\mathbf{R} + \mathbf{B}^*\mathbf{p}_{k-1}\mathbf{B}]^{-1}\mathbf{B}^*\mathbf{p}_{k-1}\mathbf{A} \tag{32}$$

The algorithm starts from $k=0$ in (32) where $\mathbf{p}_{-1} = \mathbf{0}$. Then, $\mathbf{K}_k$ is calculated as (31). $\mathbf{K}_0$ is calculated from (31) and (32) using $\mathbf{p}_{-1} = \mathbf{0}$.

Using (26) and (29), obtains the final control law

$$\begin{aligned}\mathbf{BU}_k &= \mathbf{BU}_{1k} + \mathbf{BU}_{2k} \\ &= -\left(\mathbf{I} + \mathbf{BK}_k\right)\mathbf{E}_k + \mathbf{AE}_{k-1} + \mathbf{B}\left(\mathbf{U}_{1,k-1} + \mathbf{U}_{2,k-1}\right)\end{aligned} \tag{33}$$

Since $\mathbf{U}_{1,k-1} + \mathbf{U}_{2,k-1} = \mathbf{U}_{k-1}$, final control law (33) can be represented as

$$\mathbf{BU}_k = -\left(\mathbf{I} + \mathbf{BK}_k\right)\mathbf{E}_k + \mathbf{AE}_{k-1} + \mathbf{BU}_{k-1} \tag{34}$$

To calculate $\mathbf{BU}_k$ for $k \ge 1$, $\mathbf{U}_0$ and $\mathbf{E}_0$ as initial values must be known in advance. $\mathbf{U}_0$ is given zero and $\mathbf{E}_0$ is computed from $\mathbf{E}_0 = \mathbf{X_d}(0) - \mathbf{X}(0)$ where $\mathbf{X_d}(0)$ and $\mathbf{X}(0)$ are given by the designer.

In order to calculate $\mathbf{BU}_k$ in (34) by considering $\mathbf{E} = \mathbf{X_d} - \mathbf{X}$ and $\mathbf{X} = \begin{bmatrix}\mathbf{q}\\ \dot{\mathbf{q}}\end{bmatrix}$, feedbacks of the joint positions, joint velocities and motor voltages are required. These feedbacks are $\mathbf{q}_k$, $\mathbf{q}_{k-1}$, $\dot{\mathbf{q}}_k$, $\dot{\mathbf{q}}_{k-1}$, and $\mathbf{U}_{k-1}$ which are available. In practice, measuring the voltage is common and optical encoder is conveniently used to measure the joint position and joint velocity.

5. Stability Analysis

Applying control law (33) on system (21) and using (24) results in the closed-loop system

$$\mathbf{E}_{k+1} = \left(\mathbf{A} - \mathbf{BK}_k\right)\mathbf{E}_k + \mathbf{B}\left(\mathbf{\psi}_k - \mathbf{\psi}_{k-1}\right) \tag{35}$$

Since the DLQ controller provides $\mathbf{K}_k$ such that $\mathbf{A} - \mathbf{BK}_k$ is Hurwitz, thus system (35) is stable. Then, a bounded input $\mathbf{B}\left(\mathbf{\psi}_k - \mathbf{\psi}_{k-1}\right)$ to system (35) provides a bounded output $\mathbf{E}_k$.

The boundedness of lumped uncertainty $\boldsymbol{\psi}$ is verified by the following proof.

Proof: Electrical equation of the permanent magnet dc motor is given by

$$RI_a + L\dot{I}_a + k_b\dot{\theta}_m = v \quad (36)$$

where v is the motor voltage, I_a is the motor current and $\dot{\theta}_m$ is the rotor velocity. R, L and k_b represent the coefficients of armature resistance, armature inductance, and back-emf constant, respectively.

By multiplying both sides of (36) by I_a, one can obtain the power equation

$$vI_a = RI_a^2 + L\dot{I}_a I_a + k_b\dot{\theta}_m I_a \quad (37)$$

Motor receives electrical power vI_a to produce mechanical power $k_b\dot{\theta}_m I_a$ [25]. The term RI_a^2 is the loss in the windings and the term $L\dot{I}_a I_a$ is the time derivative of magnetic energy.

Taking integral of both sides of (37) gives

$$\int_0^t vI_a dt = \int_0^t RI_a^2 dt + \int_0^t L\dot{I}_a I_a dt + \int_0^t k_b\dot{\theta}_m I_a dt \quad (38)$$

with $I_a(0) = 0$, we have

$$\int_0^t vI_a dt = RI_a^2 t + 0.5LI_a^2 + \int_0^t k_b\dot{\theta}_m I_a dt \quad (39)$$

Since $RI_a^2 t \geq 0$ and $0.5LI_a^2 \geq 0$,

$$\int_0^t k_b\dot{\theta}_m I_a dt \leq \int_0^t vI_a dt \qquad \text{for } t \geq 0 \quad (40)$$

Therefore, the mechanical energy is bounded as (40). In the other words, the electrical energy, $\int_0^t vI_a dt$ is the upper bound of mechanical energy, $\int_0^t k_b\dot{\theta}_m I_a dt$. The upper bound of mechanical energy can be calculated from (40) as

$$\int_0^t k_b\dot{\theta}_{mu} I_a dt = \int_0^t vI_a dt \qquad \text{for } t \geq 0 \quad (41)$$

where $\dot{\theta}_{mu}$ is the motor velocity at the upper bound of mechanical energy specified as $\int_0^t k_b\dot{\theta}_{mu} I_a dt$. By taking derivative of (41) with respect to time,

$$k_b\dot{\theta}_{mu} I_a = vI_a \quad (42)$$

Thus,

$$k_b\dot{\theta}_{mu} = v \quad (43)$$

Therefore, $\dot{\theta}_{mu}$ is bounded as

$$\left|\dot{\theta}_{mu}\right| \leq |v| / k_b \quad (44)$$

By using Assumption 3 one can imply that

$$\left|\dot{\theta}_{m}\right| \leq v_{max} / k_b \quad (45)$$

where v_{max} is the maximum of motor voltage limited by the voltage limiter.

From (36), it can be written that

$$RI_a + L\dot{I}_a = w \quad (46)$$

where

$$w = v - k_b\dot{\theta}_m \quad (47)$$

v is bounded as stated by Assumption 3 and $\dot{\theta}_m$ is bounded in (45). Consequently, the input w in (46) is bounded. The linear differential equation (46) is a stable linear system based on the Routh-Hurwitz criterion. Since the input w is bounded, the output I_a is bounded. From (46)

$$L\dot{I}_a = w - RI_a \quad (48)$$

$\dot{I}_a$ is bounded since w and I_a are bounded.

Result1: In summary, if the motor voltage be bounded then the motor current, I_a, its time derivative, $\dot{I}_a$, and the motor velocity, $\dot{\theta}_m$, are bounded [17]. The joint velocity, $\dot{q}$, is proportional to motor velocity, $\dot{\theta}_m$, by gear ratio. Thus, the joint velocity, $\dot{q}$, is bounded. Appling this reasoning to all motors of the robot manipulator implies that the vectors $\mathbf{I_a}$, $\dot{\mathbf{I}}_\mathbf{a}$ and $\dot{\mathbf{q}}$ are bounded.

According to properties of the robot manipulator, the following assumption can be made [26].

Assumption 4: Inertia matrix $\mathbf{D(q)}$ is bounded as

$$\lambda_{min}\mathbf{I} \leq \mathbf{D(q)} \leq \lambda_{max}\mathbf{I} \quad (49)$$

where the known positive scalars λ_{min} and λ_{max} are the smallest and largest eigenvalues of $\mathbf{D(q)}$, respectively.

Assumption 5: Matrix $\mathbf{C(q,\dot{q})}$ is bounded as

$$\left\|\mathbf{C(q,\dot{q})}\right\| \leq \zeta_c(\mathbf{q})\left\|\dot{\mathbf{q}}\right\| \quad (50)$$

where the known scalar $\zeta_c(\mathbf{q})$ is a known positive definite function of $\mathbf{q}$.

Assumption 6: Gravity vector $\mathbf{g(q)}$ is bounded as

$$\left\|\mathbf{g(q)}\right\| \leq \zeta_g(\mathbf{q}) \quad (51)$$

where $\zeta_g(\mathbf{q})$ is a known positive definite function of $\mathbf{q}$.

For revolute joint robots the scalars $\lambda_{\min}$, $\lambda_{\max}$, $\zeta_c(\mathbf{q})$ and $\zeta_g(\mathbf{q})$ are constant [26].

From (6), we have

$$\ddot{\mathbf{q}} = \left(\mathbf{J_m r}^{-1} + \mathbf{rD(q)}\right)^{-1} \mathbf{K_m R_a}^{-1}. \left(\begin{array}{l} \mathbf{V} - \mathbf{R_a K_m^{-1} r g(q)} - \mathbf{L}\dot{\mathbf{I}}_\mathbf{a} - \boldsymbol{\xi} \\ -\left(\mathbf{R_a K_m^{-1} B_m r}^{-1} + \mathbf{R_a K_m^{-1} r C(q,\dot{q})} + \mathbf{K_b r}^{-1}\right)\dot{\mathbf{q}} \end{array}\right) \quad (52)$$

One can imply the boundedness of $\ddot{\mathbf{q}}$ by considering (52). Note that in (52), $\left(\mathbf{J_m r}^{-1} + \mathbf{rD(q)}\right)$ is a positive definite matrix, thereby its inverse is available. Matrices $\mathbf{R_a}$, $\mathbf{K_m}$, $\mathbf{J_m}$, $\mathbf{B_m}$, $\mathbf{r}$, $\mathbf{K_b}$ and $\mathbf{L}$ are constant. $\boldsymbol{\xi}$ in Assumption 2, $\mathbf{V}$ in Assumption 3, $\mathbf{D(q)}$ in Assumption 4, $\mathbf{C(q,\dot{q})}$ in Assumption 5, and $\mathbf{g(q)}$ in Assumption 6 are bounded. In addition, $\dot{\mathbf{I}}_\mathbf{a}$ and $\dot{\mathbf{q}}$ are bounded in Result1. Therefore, all terms in the right hand side of (52) are bounded. Hence

Result2: $\ddot{\mathbf{q}}$ is bounded.

The boundedness of $\boldsymbol{\varphi}$ is implied by considering that all terms in the right hand side of (8) are bounded based on Assumptions 4, 5, 6, and Results 1, 2. Using (8) and Cauchy-Schwartz inequality, $\boldsymbol{\varphi}$ is bounded as

$$\|\boldsymbol{\varphi}\| \le \alpha\lambda_{\max}\|\ddot{\mathbf{q}}\| + \alpha\zeta_c\|\dot{\mathbf{q}}\|^2 + \alpha\zeta_g + \|\mathbf{L}\|\|\dot{\mathbf{I}}_\mathbf{a}\| + \boldsymbol{\xi}_{\max} = \varphi_{\max} \quad (53)$$

where $\alpha = \left\|\mathbf{R_a K_m^{-1} r}\right\|$

Result3: $\boldsymbol{\varphi}$ is bounded.

The boundedness of $\boldsymbol{\psi}$ is implied by considering that all terms in the right hand side of (10) are bounded. All matrices are constant. As implied in Results 1, 2, 3 $\dot{\mathbf{q}}$, $\ddot{\mathbf{q}}$ and $\boldsymbol{\varphi}$ are bounded. Using (10) and Cauchy-Schwartz inequality, $\boldsymbol{\psi}$ is bounded as

$$\|\boldsymbol{\psi}\| \le \beta_1\|\ddot{\mathbf{q}}\| + \beta_2\|\dot{\mathbf{q}}\| + \varphi_{\max} = \psi_{\max} \quad (54)$$

where

$$\beta_1 = \left\|\mathbf{R_a K_m^{-1} J_m r}^{-1} - \hat{\mathbf{R}}_\mathbf{a}\hat{\mathbf{K}}_\mathbf{m}^{-1}\hat{\mathbf{J}}_\mathbf{m}\hat{\mathbf{r}}^{-1}\right\|,$$

$$\beta_2 = \left\|\mathbf{R_a K_m^{-1} B_m r}^{-1} - \hat{\mathbf{R}}_\mathbf{a}\hat{\mathbf{K}}_\mathbf{m}^{-1}\hat{\mathbf{B}}_\mathbf{m}\hat{\mathbf{r}}^{-1} + \mathbf{K_b r}^{-1} - \hat{\mathbf{K}}_\mathbf{b}\hat{\mathbf{r}}^{-1}\right\|$$

Result4: $\boldsymbol{\psi}$ is bounded.

End of Proof.

The boundedness of $\boldsymbol{\psi}$ implies that $\boldsymbol{\psi}_k - \boldsymbol{\psi}_{k-1}$ is bounded. Since $\mathbf{B} = \sigma\mathbf{N}$ is a constant, $\mathbf{B}(\boldsymbol{\psi}_k - \boldsymbol{\psi}_{k-1})$ is bounded. Therefore, the stable closed-loop system (35) provides bounded output $\mathbf{E}_k$ since input $\mathbf{B}(\boldsymbol{\psi}_k - \boldsymbol{\psi}_{k-1})$ is bounded.

One can easily imply that

$$\mathbf{X}_k = \mathbf{X}_{\mathbf{d}k} - \mathbf{E}_k \quad (55)$$

Thus, the boundedness of state vector $\mathbf{X}_k$ is verified due to the boundedness of $\mathbf{E}_k$ in the closed-loop system (35) and the boundedness of desired trajectory $\mathbf{X}_{\mathbf{d}k}$ in Assumption 1.

The robust time-delay control law (26) has a main role in compensating the uncertainty. In the case of a much difference between the nominal model (28) and the actual system (27), the closed-loop system (35) is subject to a large uncertainty. The residual uncertainty in the closed-loop system (35) is reduced from a large value of $\mathbf{B}\boldsymbol{\psi}_k$ to a small value of $\mathbf{B}\left(\boldsymbol{\psi}_k - \boldsymbol{\psi}_{k-1}\right)$ due to using the robust time-delay control law (26). As a result, the performance of control system is improved by reducing the residual uncertainty. The residual uncertainty $\mathbf{B}\left(\boldsymbol{\psi}_k - \boldsymbol{\psi}_{k-1}\right)$ will be very small when the uncertainty is smooth and the sample time σ is very short.

6. Simulation Results

We simulate the proposed control law (34) on an elbow two-link revolute manipulator driven by permanent magnet dc motors, as shown in Fig. 1. The performance of controller is compared with the performance of RTOMNDR control given by [19], thus we use the same system for simulations. Details of the robot dynamics in (1) are given by

$$D(q) = \begin{bmatrix} D_{11} & D_{12} \\ D_{12} & D_{22} \end{bmatrix} \quad (56)$$

$$D_{11} = m_1 l_{c1}^2 + m_2(l_1^2 + l_{c2}^2 + 2l_1 l_{c2}\cos(q_2)) + I_1 + I_2$$

$$D_{12} = m_2(l_{c2}^2 + l_1 l_{c2}\cos(q_2)) + I_2$$

$$D_{22} = m_2 l_{c2}^2 + I_2$$

$$C(q,\dot{q}) = \begin{bmatrix} -m_2 l_1 l_{c2}\dot{q}_2\sin(q_2) & -m_2 l_1 l_{c2}(\dot{q}_1 + \dot{q}_2)\sin(q_2) \\ m_2 l_1 l_{c2}\dot{q}_1\sin(q_2) & 0 \end{bmatrix}$$

$$G(q) = \begin{bmatrix} (m_1 l_{c1} + m_2 l_1) g\cos(q_1) + m_2 l_{c2} g\cos(q_1 + q_2) \\ m_2 l_{c2} g\cos(q_1 + q_2) \end{bmatrix}$$

where q_i for $i = 1, 2$ denotes the joint angle, l_i is the link length, m_i is the link mass, I_i is the link's moment of inertia given in the center of mass, l_{ci} is the distance between the center of mass of the link and the ith joint as shown in Figure 1. The real parameters of manipulator and motors are given in Table 1 and Table 2, respectively.

Table 1. Parameters of links

I	m	l_c	l	link
5	15	0.5	1	1
2	6	0.5	1	2

Table 2. Parameters of dc servomotors

Motor	K_b	J_m	B_m	$1/r$
1	0.26	0.0002	0.000817	107.82
2	0.26	0.0002	0.00138	53.7063

The desired repetitive trajectory is given by

$$q_d = \left[\cos(0.1\pi t) \quad \cos(0.1\pi t)\right]^T \tag{57}$$

$$P_d = \begin{bmatrix} \cos\left(\cos(0.1\pi t)\right) + \cos\left(\cos(0.1\pi t) + \cos(0.1\pi t)\right) \\ \sin\left(\cos(0.1\pi t)\right) + \sin\left(\cos(0.1\pi t) + \cos(0.1\pi t)\right) \end{bmatrix} \tag{58}$$

where q_d is a vector of desired joint angles to provide the desired end point position in x-y plane denoted by P_d. The end-point of robot goes and returns along the path. These two parts of trajectory obtain a cycle of period trajectory with a period of $20S$. The desired trajectory is sufficiently smooth and the motors are strong enough such that the robot can track the desired trajectory. We run the simulations for two periods to illustrate the repetitive motion.

The uncertainty may include the external disturbances, unmodeled dynamics, and parametric uncertainty. To consider the parametric uncertainty, all parameters of the nominal model used in the control law are given as 95% of the real one. The external disturbance is given to the input of each motor as a random signal with the maximum value $+4V$ and the minimum value $-4V$ with a period of $2S$. The unmodeled dynamics is considered through the motor inductances that are not included in the nominal model. The uncertainty is unknown; however, we have to use an example of a bounded uncertainty to check the performance of the control system. The matrices $\mathbf{Q}$ and $\mathbf{R}$ in (27) and (28) are given by $\mathbf{Q} = 10^8 \mathbf{I}_{4\times4}$ and $\mathbf{R} = \mathbf{I}_{2\times2}$ where $\mathbf{I}_{n\times n}$ is the $n \times n$ identity matrix.

Simulation1: The initial position of the end point is set to $P(0) = [1 \quad 1]m$ in the $x-y$ plane while the initial position of the desired trajectory is given by $P_d(0) = [0.1242 \quad 1.7508]m$. The initial error is calculated as $P_d(0) - P(0) = [-0.8758 \quad 0.7508]$. As a practical regard the motor voltages are limited to the maximum value of 40 V to protect the motors from over voltages. The end-point starts from initial point and after $6S$ reaches to the desired path as shown in Figure 2. The task is repeated two times in $40S$. The norm of tracking errors is vanished well after $6S$ and comes under the $2.26 \times 10^{-4} m$ at the end in Figure 3. The motor voltages are under the permitted value of 40V and behave well without any problems, as shown in Figure4. The jumps on the control efforts confirms that the control effort promptly reply to the external disturbances. As a result, the uncertainties are compensated well.

Simulation 2. The control system is simulated with the zero initial error. The tracking error is ignorable with the maximum value of about $e_x = 2.46 \times 10^{-4} m$ and $e_y = 2.1 \times 10^{-4} m$ as shown in Figure 5 and

The control efforts behave well under the permitted value of $40V$ and promptly reply to the external disturbances as shown in Figure 6.

Simulation 3: A comparison is presented between the proposed method and the RTOMNDR control.

All conditions including the initial errors are given the same as simulation 1 for comparing the results. The RTOMNDR has used a linear discrete time-variant nominal model for the robotic system. The model is dependent on the manipulator dynamics and motors' parameters. Then, a robust time-delay controller has been used to compensate differences between the actual system and nominal model. Finally, a time-optimal minimum-norm controller is applied to locate the poles of discrete system at the origin of complex plane. The tracking performance is very well such that the norm of tracking errors is vanished well after $1S$ and comes under the $3.2 \times 10^{-4} m$ at the end in Fig. 7. The control efforts jump to the maximum values when starting, then behave well under the permitted values as shown in Fig. 8.

Comparing the results shows that both controllers present competitive tracking performances. The tracking errors decrease faster in the RTOMNDR controller whereas the control efforts jump to the maximum values. In contrast, the control efforts of the RODR behave smoother and tracking errors reduce much more at the end. The RTOMNDR control is computationally extensive and depends on the manipulator dynamics whereas the RODR is free from manipulator dynamics, thus is computationally simple.

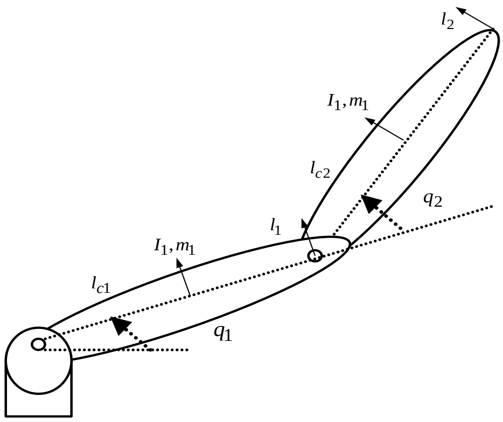

Fig. 1. Two-link elbow manipulator

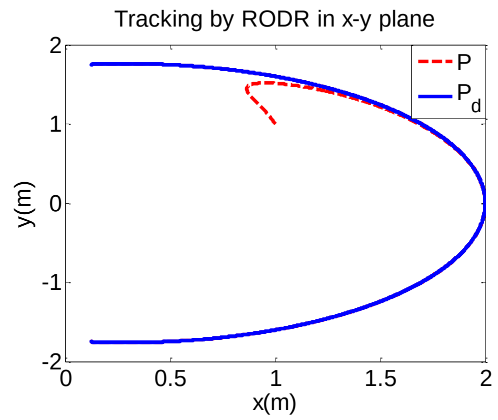

Fig. 2.Tracking by RODR control in the x-y plane

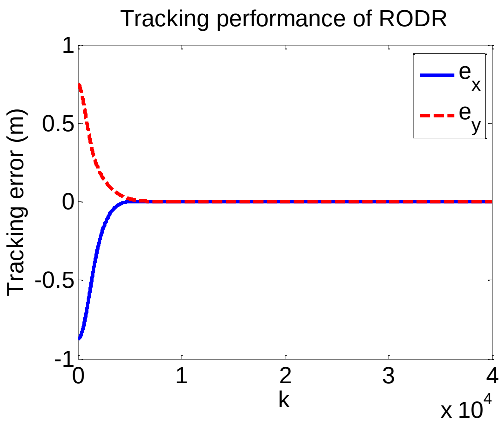

Fig. 3. Tracking performance

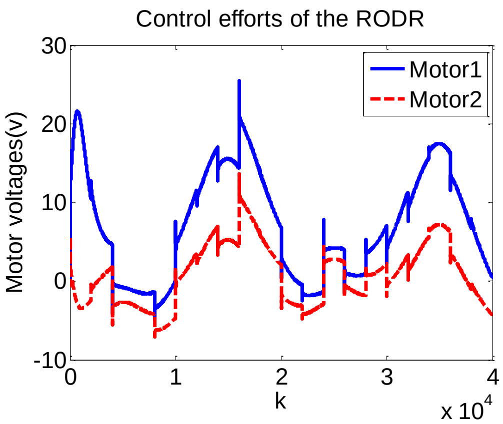

Fig. 4. Control efforts of the RODR control

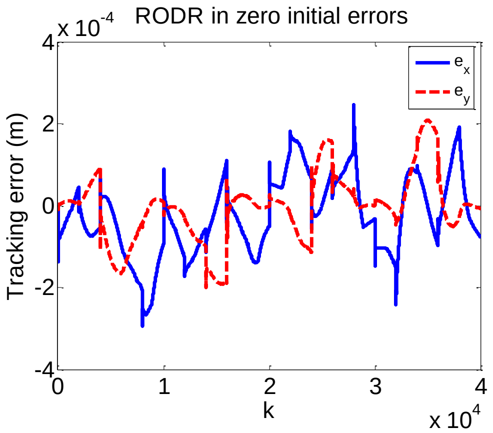

Fig. 5. RODR control without initial error

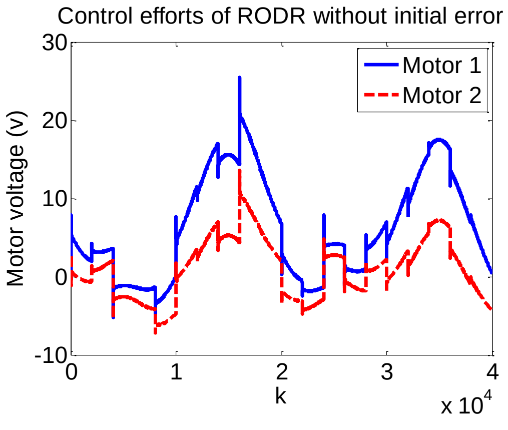

Fig. 6. Control efforts without initial error

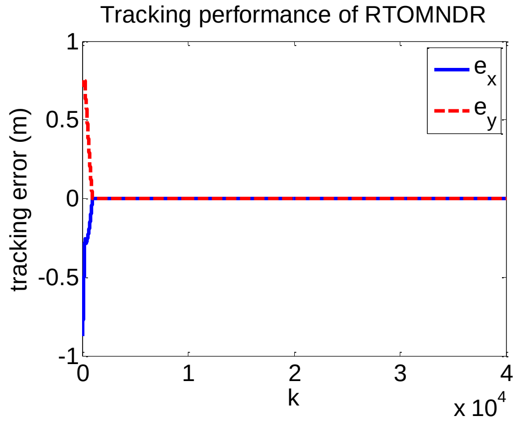

Fig. 7. RTOMNDR control in initial error

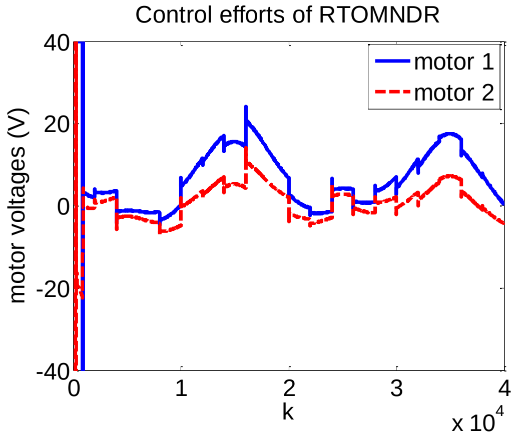

Fig. 8. Control efforts of RTOMNDR control

We have noticed that the nonlinearity, coupling and uncertainty in the robot dynamics is a challenge in applying the DLQ control. For this purpose, the voltage control strategy has been efficiently used to obtain a discrete linear time invariant system which is free from manipulator dynamics.

7. Conclusions

All nonlinearities and uncertainties have been considered as a lumped uncertainty in the model. Then a robust time-delay control has been employed to compensate the lumped uncertainty. As a result, a suitable discrete linear time-invariant model has been obtained to apply efficiently the DLQ control. The closed-loop system is stable according to the stability analysis while an optimal tracking performance by the DLQ control is provided and the robustness of control system in the presence of uncertainties is guaranteed using the robust time-delay controller. The control system can overcome a wide range of uncertainty including external disturbances, parametric uncertainty and unmodeled dynamics.

The performance of robust time-delay control is highly improved if the uncertainty is smooth and the sampling period is sufficiently short. A comparison shows that the proposed controller is much simpler and much less computational than the RTOMNDR since it is free from manipulator dynamics. Its control efforts behave smoother than the RTOMNDR, however, the RTOMNDR is relatively faster than the proposed controller.

Reference

[1] Tsai MC, Anwar G, Tomizuka M (1988) Discrete time repetitive control for robot manipulators. IEEE International Conference on Robotics and Automation, Philadelphia 3: 1341–1346.

[2] Tsai MC, Tomizuka M (1989) Model reference adaptive control and repetitive control for robot manipulators. Proc. IEEE International Conference on Robotics and Automation 3: 1650–1655.

[3] Dixon WE, Zergeroglu E, Dawson DM, Costic, BT (2002) Repetitive learning control: A Lyapunov-based Approach. IEEE Transactions on Systems, Man, and Cybernetics, Part B: Cybernetics 32(4): 538–545.

[4] Sun M, Ge SS, Mareels IMY (2006) Adaptive repetitive learning control of robotic manipulators without the requirement for initial repositioning. IEEE Transactions on Robotics 22(3): 563–568.

[5] Arimoto S (1990) Learning control theory for robotic motion. Int J Adapt Control 4(6): 543–564.

[6] Sun M, Wang D (2001) Initial condition issues on iterative learning control for nonlinear systems time delay. Int J Syst Sci 32(11): 1365–1375.

[7] Wen C, Deman L (1996) A learning control for a class of nonlinear systems with exogenous disturbances. Int J Syst Sci 27(12): 1453–1459.

[8] Zhang B, Wang D, Ye Y (2010) On learning transient, auto-tuning of learnable bandwidth and lead step in iterative learning control. Int J Syst Sci 41(4): 353–363.

[9] Roh CL, Lee MN, Chung MJ (1996) ILC for Non-minimum phase systems. Int J Syst Sci 27(4): 419–424.

[10] Sadegh N, Horowiz R, Kao WW, Tomizuka M (1990) A united approach to the design of adaptive and repetitive controllers for robotic manipulators. ASME Journal of Dynamic System, Measurement and Control 112(4): 618–629.

[11] Messener W, Horowitz R, Kao WW, Boals M (1991) A new adaptive learning rule. IEEE Transaction on Automatic Control 36(7): 188–197.

[12] Kaneko K, Horowitz R (1997) Repetitive and adaptive control of robot manipulators with velocity estimation. IEEE Transaction on Robotics and Automation 13(2): 204–217.

[13] Tayebi A (2004) Adaptive iterative learning control for robot manipulators. Automatica 40: 1195–1203.

[14] Fateh MM (2008) On the voltage-based control of robot manipulators. International Journal of Control, Automation, and Systems 6(5): 702–712.

[15] Fateh MM (2010) Robust fuzzy control of electrical manipulators. Journal of Intelligent Robotic Systems 60(3-4): 415–434.

[16] ateh MM (2010) Robust voltage control of electrical manipulators in task-space. Int J Innov Comput I 6(6): 2691–2700.

[17] Fateh MM (2012) Robust control of flexible-joint robots using voltage control strategy. Nonlinear Dynamics 67(2): 1525–1537.

[18] Fateh MM (2012) Nonlinear control of electrical flexible-joint robots. Nonlinear Dynamics 67(4): 2549–2559.

[19] Fateh MM, Ahsani Tehrani H, Karbassi SM (2013) Repetitive control of electrically driven robot manipulators. Int J Syst Sci 44(4): 775–785.

[20] Fateh MM, Khorashadizadeh S (2012) Robust control of electrically driven robots by adaptive fuzzy estimation of uncertainty. Nonlinear Dynamics 69(3): 1465–1477.

[21] Spong MW, Hutchinson S, Vidyasagar M (2006) Robot modeling and control, 1st Edition, Wiley.